Mechanics of Materials 17 (1994) 155–164
Elsevier

Characteristics and microstructure in the evolution of shear localization in Ti–6Al–4V alloy

Yilong Bai [a], Qing Xue [a], Yongbo Xu [b] and Letian Shen [a]

[a] *Laboratory for Non-linear Mechanics of Continuous Media, Institute of Mechanics, Chinese Academy of Sciences, Beijing, 100080, China*

[b] *Laboratory of Fatigue and Fracture for Materials, Institute of Metal Research, Chinese Academy of Sciences, Shenyang, 110015, China*

Received 16 September 1992; revised version received 12 February 1993

A new interrupting method was proposed and the split Hopkinson torsional bar (SHTB) was modified in order to eliminate the effect of loading reverberation on post-mortem observations. This makes the comparative study of macro- and microscopic observations on tested materials and relevant transient measurement of $\tau-\gamma$ curve possible.

The experimental results of the evolution of shear localization in Ti–6Al–4V alloy studied with the modified SHTB are reported in the paper. The collapse of shear stress seems to be closely related to the appearance of a certain critical coalescence of microcracks. The voids may form within the localized shear zone at a quite early stage. Finally, void coalescence results in elongated cavities and their extension leads to fracture along the shear band.

1. Introduction

In the recent twenty years, the study of the evolution of shear localization has drawn great attention. Numerous works in theoretical analysis and numerical simulations have been performed to predict the process of shear localization and to determine the factors governing the process (Bai, 1982; Clifton et al., 1984; Bai et al., 1986; Wright and Batra, 1987; Shawki and Clifton, 1989 and Xing et al., 1991). Noticeablely, a number of scaling laws have been obtained (Backman et al., 1986; Bai, 1989; Bai et al., 1990; Anand et al., 1990). But "analysis of localized plastic shearing deformation is currently limited by a lack of critical comparisons of theory and experiment" (Anand et al., 1990). In the light of the situation, some experimental attempts to measure the process of shear localization have been made. Costin et al. (1979) and Hartley et al. (1987) measured the temperature history of shear localization. Marchand and Duffy (1988) improved their infrared technique and measured the temperature distribution and history. Giovanola (1988) and Marchand and Duffy (1988) separately observed the transient deformation field in the process of shear localization by means of high speed photography and a grid pattern. All these works certainly blazed a trail in the experimental study of the process of shear localization, but the methods could not reveal the evolution of microstructure during shear localization and, hence, could not clarify the relation of shear banding to the loss of strength. In particular, "a critical need is for an improved understanding of the relation of localization to the microstructure of the material. This is a many faceted issue ranging from the effect of the initial microstructure on the early stages of deformation leading to instability, through changes in microstructure occurring during localization, to the microstructures which result after the shear band formation is completed. Throughout the process the evolving microstructure determines the material response that needs to be

Correspondence to: Prof. Yilong Bai, Laboratory for Non-linear Mechanics of Continuous Media, Institute of Mechanics, Chinese Academy of Sciences, Beijing, 100080, China.

SSDI 0167-6636(93)E0064-9

considered in the formulation of constitutive models for the analysis and design of the many processes in which shear band is an important design consideration" (Anand et al., 1990). In order to meet this need, Xue et al. (1992) proposed a new experimental interrupting method and modified the split Hopkinson torsional bar (SHTB) to eliminate the effect of loading reverberation on post-mortem observations. This new experimental technique makes the comparative study of macro- and microscopic observations on tested materials and relevant transient measurement of $\tau-\gamma$ curves possible.

This paper reports the experimental results of the evolution of shear localization in Ti-6Al-4V alloy, a material very sensitive to shear banding. A series of tests have been carried out with the modified SHTB to investigate the evolving microstructure in shear localization at a strain rate of about 310 s^{-1}. Then the post-mortem observations of specimens tested to different plastic deformation unveil the relation between the microscopic characteristics in the localization process and the transient $\tau-\gamma$ curve.

2. Experimental procedure

It is very difficult to look at evolving microstructure during the process of shear localization under dynamic loading, because of the transient nature of the process and the localizing field. However, if the deformation and evolving microstructures in the process can be "frozen" in the specimen in the order of loading durations, the post-mortem observation of tested specimens can provide the clue to the macro- and microscopic characteristics in this process, then establishing their correlation to transient measurement of $\tau-\gamma$ will become possible. According to this idea, a method of interrupting the SHTB test was put forward. Concretely, the performance of the

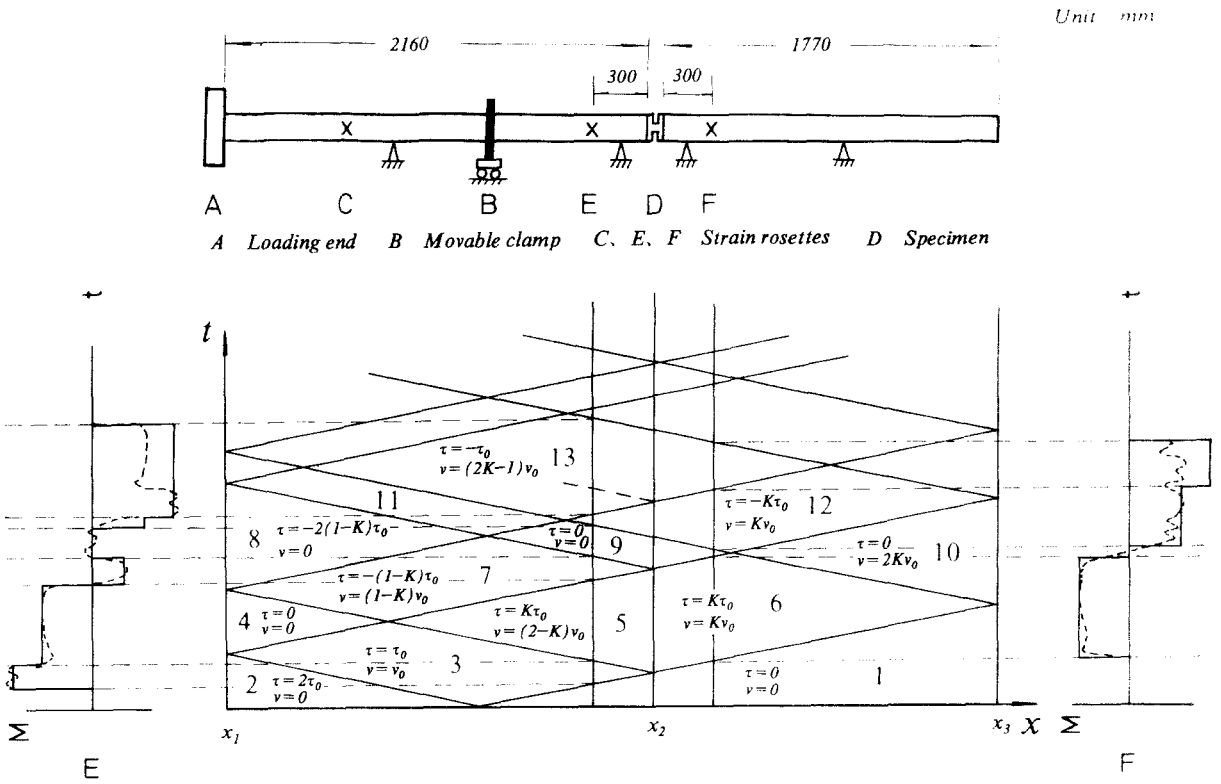

Fig. 1. Split Hopkinson torsional bar apparatus and its wave analysis.

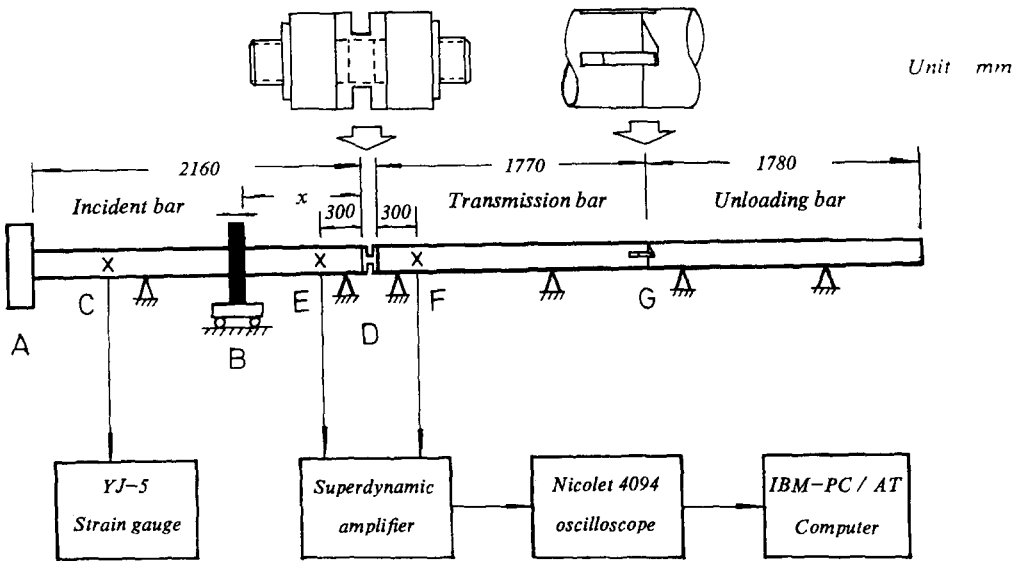

A Loading end B Movable clamp C, E, F Strain rosettes D Specimen G Connector

Fig. 2. Modified SHTB apparatus.

interrupting test on the SHTB is as follows. With a specified loading amplitude and identical specimens, a set of tests are carried out under different loading durations, which can be realized by finely and accurately adjusting the position of the clamp of the SHTB. Hence, the group of tested specimens with different relics of localized deformation in the order of loading durations can be used in the study of the evolving microstructure during shear localization.

But, the usual SHTB has a major disadvantage preventing the planned study. This is the reverberation of torsional waves due to wave reflection at the bar ends (see Fig. 1). The reverberation of torsional waves results in secondary and reverse loadings on the specimen after the first loading. Therefore, the post-mortem features will be the result of the multi-loadings. This obscures the true microstructure from the first torsional wave. Clearly, these post-mortem features cannot be applied to correlate to the transient $\tau \sim \gamma$ measurements. Xue et al. (1992) modified the usual SHTB by attaching an unloading bar and an inside-pushed connector. In this way, the transmission wave is led out of the loading system after the first loading, while the reflected wave is controlled below a certain limit. Therefore, the modified SHTB can ensure that no secondary plastic deformation is imposed on the specimen after the first torsional wave pulse.

The modified SHTB and recording system used in the present experiments are shown in Fig. 2. The clamp can move forward and backward along rails to provide fine and accurate loading duration adjustment. More significantly, when the in-

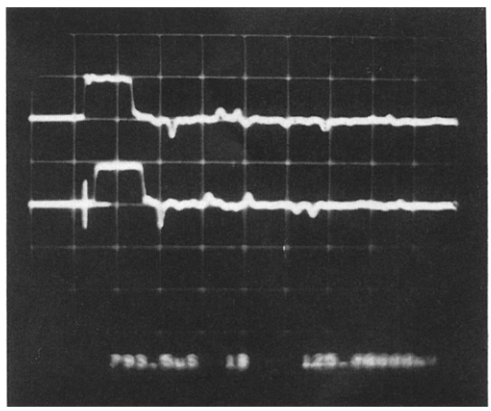

Fig. 3. The oscillogram with a dummy specimen, showing single torsional loading pulse with the modified SHTB.

Fig. 4. Optical micrograph of structure of treated Ti-6Al-4V alloy.

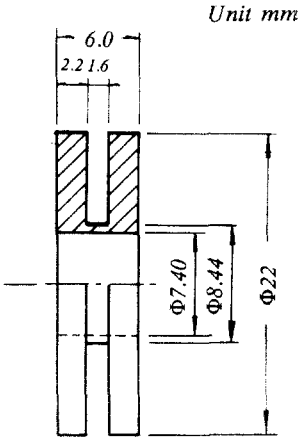

Fig. 5. Profile and dimensions of the specimen.

put loading pulse has passed though the specimen completely, the connector between the transmission and the unloading bars will automatically separate the two bars in a timely manner. This is realized by the special design of the inside-pushed connector and the difference of rotational speeds of the two bars. The details of working principle, design and test of the modified SHTB can be found in Xue (1991).

The calibration of the apparatus was fulfilled in a routine way to guarantee accurate control of loading torque, duration and the elimination of loading reverberation. Figure 3 shows the achieved single loading pulse with the modified SHTB. This satisfies the prerequisite to the reliability of our comparative study of the microstructure in the evolution of shear localization and the transient $\tau-\gamma$ measurement.

A hot-rolled Ti-6Al-4V alloy was tested in the present study. Its chemical composition is shown in Table 1. The hot-rolled bar was treated as a solid solution i.e. annealed at 980°C for one hour and then air-cooled. Its microstructure appears to be laminar $\alpha + \beta$ phase colonies (Fig. 4). Within the β phase there are grain of about 400 μm, while groups of α phase keep the uniform orientation.

A two flange thin wall tube specimen was used in these tests (see Fig. 5). It is 1.6 mm long in gauge length, 7.4 mm in internal diameter and 0.5 mm in wall thickness. The circular flanges were designed to match the torsional impedance of the aluminium bars. Both inside and outside walls of the thin wall tube were finely machined to remove surface defects. Several scribe lines were drawn on the inside surface to facilitate post-mortem observations.

After torsional testing, the specimens with localized deformation were sectioned by spark machining and prepared through standard metallographic grinding, polishing and etching methods. The etching solution consisted of 20% HF, 20% HNO_3 and 60% H_2O. The gauge sections of specimens were examined with both optical and scanning electron microscopes. Microstructures of foil specimens were also examined with a Philips EM 420 transmission electron microscope.

Table 1
Chemical composition of the tested Ti-6al-4V alloy

Alloying elements (%)			Impurity (%) less than						
Al	V	Ti	Fe	Si	C	N	H	O	rest
5.5-6.8	3.5-4.5	rest	0.30	0.15	0.10	0.05	0.015	0.20	0.40

3. Experimental observations and results

A series of tests have been performed on the modified SHTB at average strain rates of about 310 s^{-1}. Then the deformed inside scribe lines on the tested specimens were examined. After polishing and etching, the metallographical observations of the same site of gauge section were made. TEM examinations were also made to understand the configuration of dislocations.

Figure 6 shows four stress–strain curves with four prescribed loading durations labelled T9-38, T9-39, T9-37 and T9-21. Noticeably, these tests show that there is a climax in the τ–γ curves. The average critical strain is about 0.166, corresponding to a loading time of 468 μs. T9-38 was loaded 450 μs, close to the critical time, showing a maximum strain of 0.160, so that it can represent the state near the critical point. Its inside scribe lines do show homogeneous deformation without any kinks over the whole gauge length. So does its microstructure. Beyond the critical point, the stress drops slowly. Specimen T9-39, loaded to about 550 μs, attained a nominal strain of 0.196 before unloading. Its scribe lines show some hints of inhomogeneous deformation. Close-up metallographic observation displays the distinct occurrence of shear localization within the grains but transgranular tendency of localized shear (see Fig. 7). The width of the local shear zone is about 44 μm and the maximum shear strain there comes to about 1.07, 5 times the average value. A tiny elliptical void can be seen within the shear zone. Its major axis of about 6 μm is along the shear direction. More interestingly, the width of the local shear zone is much less than the size of the grain, but its extension covers several grains. Loaded to 650 μs, specimen T9-37 gained a nominal strain of 0.219. Severe localized shear band can be noticed even with naked eyes. Figure 8 exhibits a drastic change of the microstructure in the localized shear zone. Obviously, microvoids have grown and some of them have coalesced into large cracks, even extended from one grain to another, but there are still some segments not cracked in the shear band. The width of the shear band and the localized strain are uneven along the shear band. Near the crack tip, the shear band is 20 μm wide attaining a strain of 2.14, whereas apart from the crack zone it has a strain

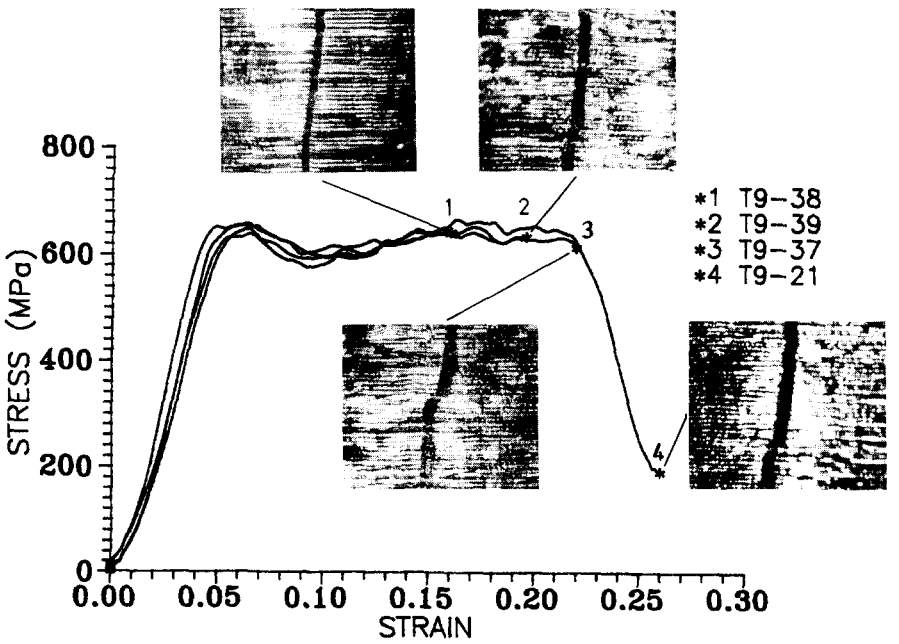

Fig. 6. Four stress–strain curves and the corresponding pattern of inside scribe lines.

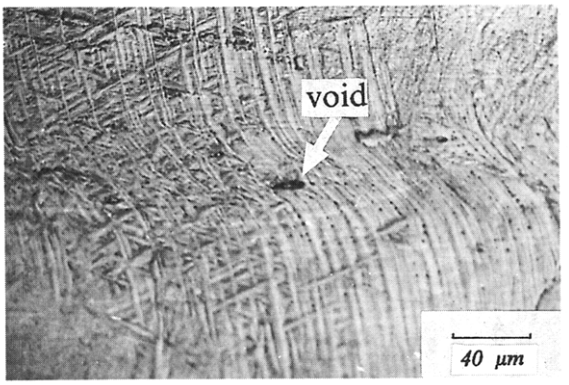

Fig. 7. Distinct zone of shear band with void.

of 1.07 and width of about 60 μm. Informatively, the distinct shear band with even partly linked cracks does not significantly affect the capacity of the material to continue supporting the load (point 3 in Fig. 6). In fact, the steep drop of shear stress can only appear after a loading of 660 μs. Specimen T9-21, with a loading duration of 750 μs, presents a greater average strain of 0.26, but much lower stress, only one-third of that at the critical point. Figure 9 displays the morphology of the localized zone. A thin and lengthy macrocrack along the shear band has formed. On each side of the crack there are clear twist zones of α-phase colonies. Its half width is about 10 μm.

Another feature of the extension of the shear band is displayed in test T9-20 (see Figs. 10a and 10b). In Fig. 10a, a distinct shear band of 25 μm width with a number of voids and a microcrack, has attained a local strain 3.7. Why such severe local strain has not made the test piece fail is a puzzle. Figure 10b was taken on the same region of specimen T9-20, but with a large field of view. In the picture, there is a secondary local shear zone of 40 μm wide and local strain 2.7 beneath the first one. Following the shear bands circumferentially, one can find that the secondary band is the tail of the primary one after its extending over the whole circumference of the tubular specimen. This is an additional fact showing the inhomogeneous strain around the circumference and the deviation of orientation of the shear band.

Usually, the sudden drop in the $\tau-\gamma$ curve was described as catastrophic failure due to the presence of the shear band (Marchand and Duffy, 1988). However, the comparative examination of T9-39, 37, 21 and the $\tau-\gamma$ curve (Fig. 6) seems to us that the decisive mechanism governing the loss of load-carrying capacity is the shear band induced successive coalescence of microcracks

Fig. 8. Shear band with voids and microcracks.

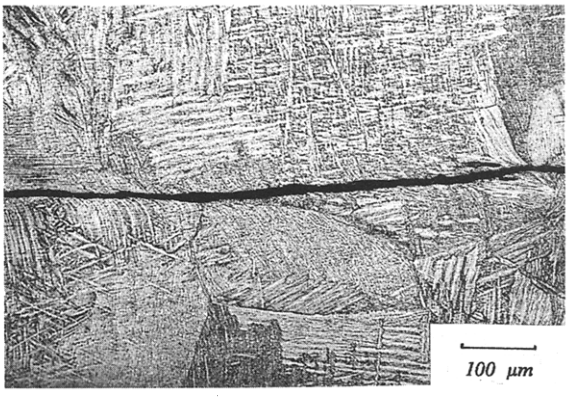

Fig. 9. Coalescence of microcracks in localized zone.

Fig. 10a. The main shear band with voids and microcracks.

around the circumference with increasing loading time, rather than the shear band itself. This is in fair agreement with calculation of a late stage behaviour of a shear band (Bai, 1989; Bai et al., 1987). On the other hand, the parabolic dimples on the fracture surface are the relic of elongated

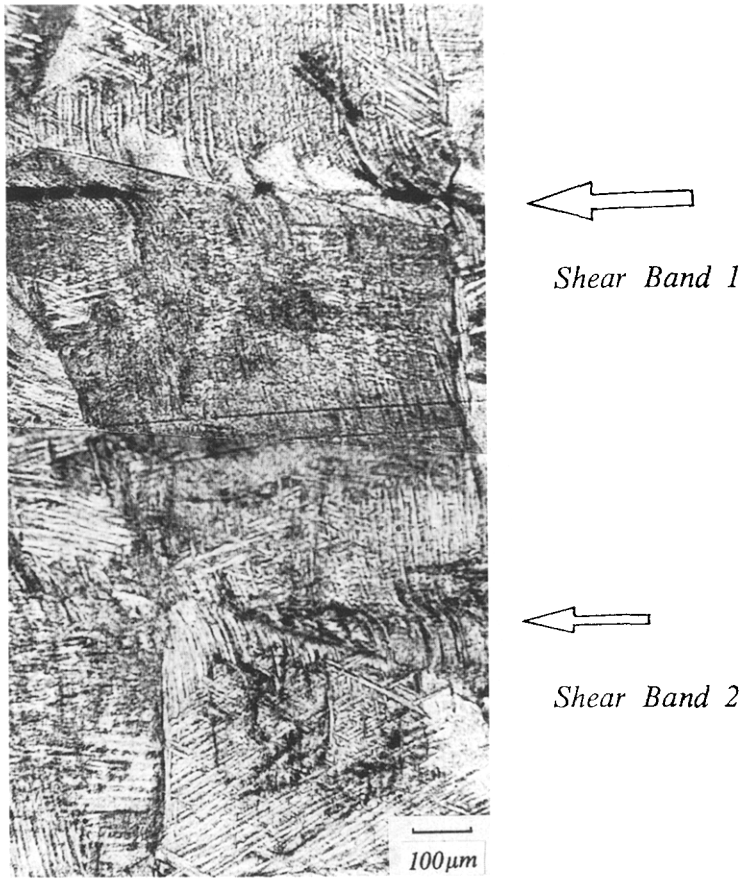

Fig. 10b. Two shear bands over the same section of specimen.

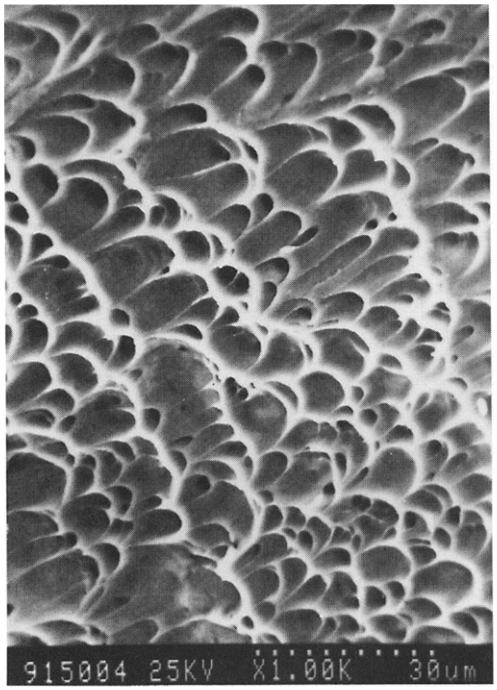

Fig. 11. Paraboloid dimple region in Ti–6Al–4V alloy.

and coalesced voids during failure (Fig. 11) and should be an additional corroboration of the process.

The estimation of the temperature rise within the shear band was conducted according to an adiabatic assumption. If the shear stress and strain were assumed to be 620 MPa and 3.73, both are the maximum values in our tests, the temperature rise should be 852°C, lower than the transformation temperature of 950°C. In fact, no phase transformation was observed within the shear band zone in these tests.

Although the shear bands are of deformed type, the shear band induced microstructural change is still recognizable. In particular, Fig. 12 shows numerous dislocations in a shear band within a grain. Distinctively, parallel to shear direction there are several dislocation walls, emanating and absorbing dislocations. Therefore, there are a number of movable dislocations in the channel between two parallel dislocation walls (Fig. 13). Obviously, this is a shear band induced configuration of dislocations. Perhaps, it might be

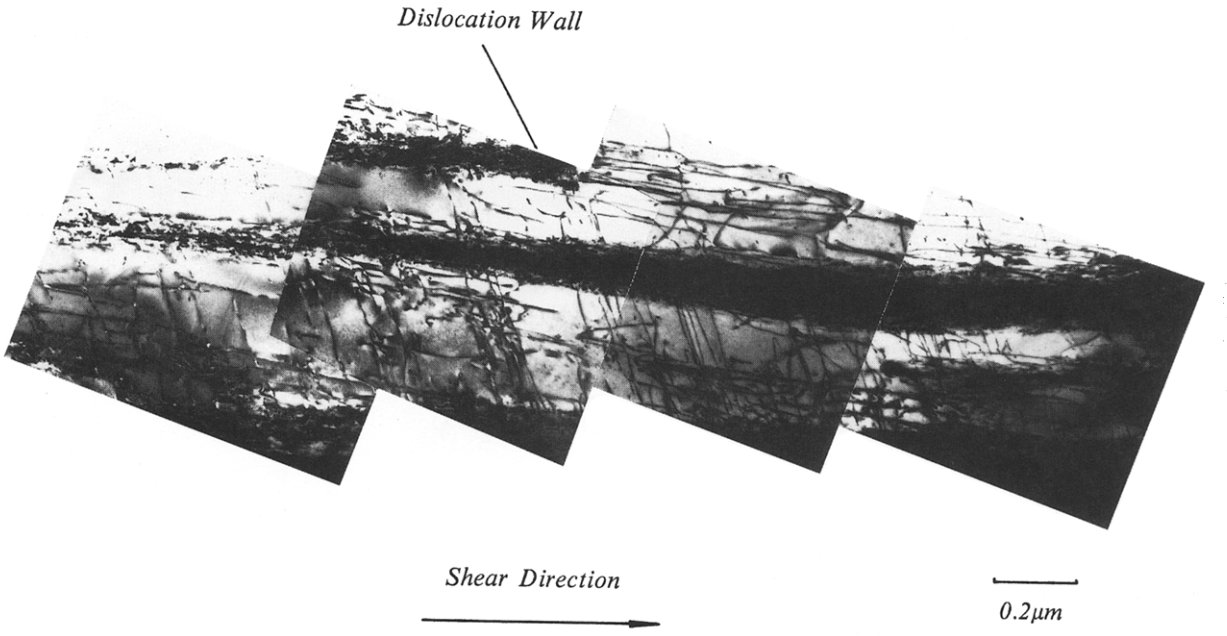

Fig. 12. Dislocation wall structure with heavy density of dislocations in the shear band.

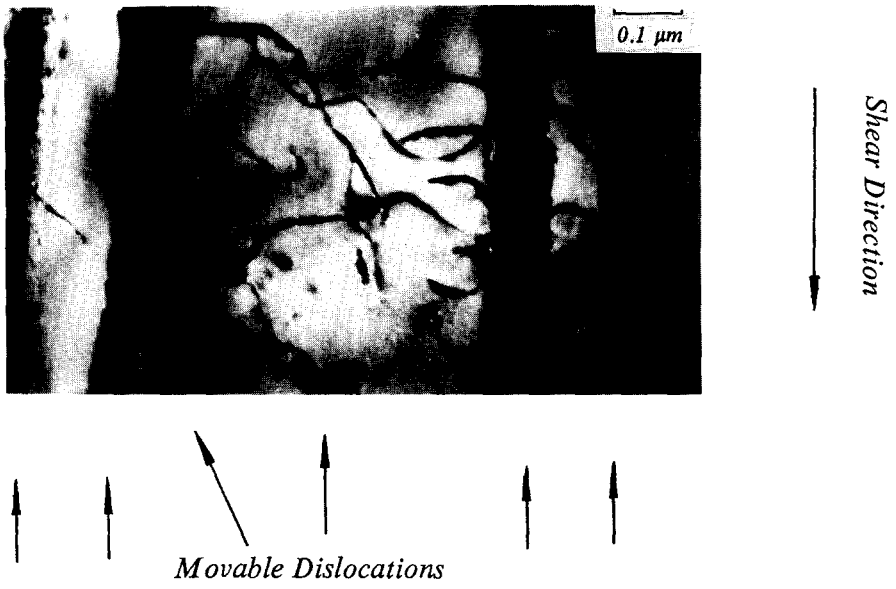

Fig. 13. Movable dislocations within the channel.

this microscopic mechanism supporting the shear band, though narrower than the grain size, that causes it to penetrate into adjacent grains. Further TEM observation and analysis is underway.

4. Conclusions

The evolution of shear localization in Ti-6Al-4V was investigated by means of an interrupting test method and the modified SHTB. The

Table 2
Results and comparison

No. specimen	Loading duration (μs)	Average strain	Localized strain	Band width (μm)	Feature of scribe lines	Microstructure observation	Position on $\tau-\gamma$ curve	Ref.
T9-38	450	0.160	–	–	homogeneous	no localized zone	near the critical strain (0.166, 468 μs)	Fig. 6
T9-39	550	0.196	1.07	44	inhomogeneous	SB [a] with void	drop slowly	Figs. 6 and 7
T9-37	650	0.219	1.07-2.14	20-40	localized zone	SB with partly linked cracks	near the steep drop (~660 μs)	Figs. 6 and 8
T9-21	750	0.260	2.75	20	localized zone with cracks	coalescent cracks along SB	only one-third of the stress at critical point	Figs. 6 and 9

[a] SB – shear band.

"frozen" localized deformation in the specimens was examined through post-mortem macro- and microscopic observation of shear bands. The main points are outlined as follows (see Table 2):

(1) Deformed shear bands were found in Ti–6Al–4V alloy at a strain rate of 310 s^{-1}. The band width is about 20–40 μm.

(2) The observations of scribe lines and the material microstructure indicate that the deformation over the gauge length keeps nearly homogeneous at the critical point of the $\tau-\gamma$ curve.

(3) From the critical point to fracture, shear bands form within grains but tend to develop transgranularly.

(4) The development of a distinct shear band, with even partly linked cracks, does not affect severely the capacity of the material to support load.

(5) The collapse of shear stress seems to be closely related to the appearance of a certain critical coalescence of microcracks, rather than to the presence of the shear band.

(6) The voids may be formed within the localized shear zone at a quite early stage. Their sizes are compatible with the width of the shear band. Finally, void coalescence results in elongated cavities and their extension leads to the fracture along the shear band.

(7) The high density of dislocations and the presence of a dislocation wall structure within the bands seems to be responsible for the highly localized shear deformation.

Acknowledgements

The work is granted by the Chinese National Natural Science Foundation. The first author (Y. Bai) also wish to thank the U.S. Army Research Office for the invitation to present this paper at the 29th SES Annual Technical Meeting.

References

Anand, L., O. Dillon, T.A. Place and B.F. Von Turkovich, (1990), Report of the NSF workshop on Localized Plastic Instabilities and Failure Criteria, *Int. J. Plast. 6(2)*, I–IX.

Backman, M.E. S.A. Finnegan, J.C. Shulz and J.K. Pringle (1986), Scaling rules for adiabatic shear, in: L.E. Mur, K.P. Staudhammer and M.A. Meyers, eds., *Metallurgical Applications of Shock-Wave and High-Strain-Rate Phenomena*, Marcel Dekker, New York and Basle, p. 675.

Bai, Y. (1982), Thermo-plastic instability in simple shear, *J. Mech. Phys. Solids 30*, 195.

Bai, Y.L. (1989), Evolution of thermo-visco-plastic shearing, in: J. Harding, ed., *Mech. Prop. Materials at High Rates of Strain*, IOP Publishing Ltd., Bristol, p. 99.

Bai, Y.L., C.M. Cheng and Y.S. Ding (1987), Development of thermoplastic shear band in simple shear, *Res. Mech. 22*, 313.

Bai Yilong, Cheng Chemin and Ling Zhong (1990), Localization and pattern of deformation in thermo-visco-plastic material, presented at Int. Conf. Mech. Phys. and Structure of Materials, Thessaloniki, Greece.

Bai Yilong, Cheng Chimin and Yu Shanbing (1986), On evolution of thermo-plastic shear band, *Acta Mech. Sinica 2*, 1.

Clifton, R.J., J. Duffy, K.A. Hartley and T.G. Shawki (1984), On critical conditions for shear band formation at high strain rates, *Scripta Metall. 18*, 443.

Costin, L.S., E.E. Crisman, R.H. Hawley and J. Duffy (1979), On the localization of plastic flow in mild steel tubes under dynamic torsional loading, in: J. Harding, ed., *Proc. 2nd Conf. on Mechanical Properties at High Rates of Strain*, Institute of Physics, Bristol and London, p. 90.

Giovanola, J.H. (1988), Adiabatic shear banding under pure shear loading – part 1: Direct observation of strain localization and energy dissipation measurements, *Mech. Mater. 7*, 59.

Hartley, K.A., J. Duffy and R.H. Hawley (1987), Measurement of the temperature profile during shear band formation in steels deforming at high strain rates, *J. Mech. Phys solids 35*, 283.

Marchand, A. and J. Duffy (1988), An experimental study of the formation process of adiabatic shear bands in a structural steel, *J. Mech. Phys. Solids 36*, 59.

Shawki, T.G. and R.J. Clifton (1989), Shear band formation in thermal viscoplastic materials, *Mech. Mater. 8*, 13.

Wright, T.W. and R.C. Batra (1987), Adiabatic shear bands in simple and dipolar plastic materials, in: K. Kawata and J. Shioiri, eds., *Proc. IUTAM Symposium on Marco- and Micro-mechanics of High Velocity Deformation and Fracture*, Springer, Berlin, p. 189.

Xing, D., Y.L. Bai, C.M. Cheng and X.L. Huang (1991), On the post-instability process of adiabatic shear, *J. Mech. Phys. Solid 39*, 1017.

Xue Qing (1991), An experimental study of evolution of thermovisco-plastic and shear localization in Ti–6Al–4V alloy and No. 20 steel, Thesis, Institute of Mechanics, Academia Sinica.

Xue, Q., Y. Bai and L. Shen (1992), Modified SHTB and its application to microscopic study of thermo-visco-plastic shear localization, in: *Proc. 2nd Int. Symp. on Intense Dynamic Loading and Its Effects*, Chengdu, China, p. 405.